Thermoresponsive viscosity of polyacrylamide block copolymers synthesised *via* aqueous Cu-RDRP

Fehaid Alsubaie,*[1,2] Evelina Liarou,[1] Vasiliki Nikolaou,[1, 3] Paul Wilson[1] and David M. Haddleton*[1]

1. *Department of Chemistry, University of Warwick, Coventry, CV4 7AL, UK*
2. *National Centre for Petrochemicals Technology, King Abdulaziz City for Science and Technology (KACST), P.O. Box 6086 Riyadh 11442, Kingdom of Saudi Arabia*
3. *Medherant Ltd, University of Warwick Science Park, Coventry CV4 7EZ*

Keywords: Thermoresponsive: Polyacrylamide block copolymers: Cu-RDRP

Abstract

Aqueous Cu-RDRP was utilized for the rapid synthesis of poly(*N*-isopropyl acrylamide)-*block*-poly(2-hydroxyethyl acrylamide) (PNiPAm$_x$-*b*-PHEAAm$_y$) copolymers with thermo-responsive viscosity. The pre-disproportionation of Cu(I)Br in the presence of an aliphatic tertiary amine (Me_6Tren) in water generated *nascent* Cu(0) and [Cu(II)] complexes and facilitated the rapid synthesis of a series of (block) copolymers with low dispersity values ($1.08 < Đ < 1.22$) and control over the molecular weight ($M_{n,SEC}$ ~30,000). The control over the polymerization enabled the design of a series of block copolymers with precision over the segment ratio, which exhibit different thermo-responsive aggregation. Thermal analysis, viscometry and fluorescence measurements gave insights on the effect of composition and temperature alterations rendering the synthesized polymers potential candidates for temperature-dependent applications.

Introduction

Over the last few decades, the rapid development of reversible deactivation radical polymerization (RDRP) has become increasingly important in polymer synthesis. The different RDRP techniques, namely transition metal-catalyzed controlled/"living" radical polymerizations,[1-5] reversible addition-fragmentation chain transfer radical polymerization (RAFT),[6-8] nitroxide-mediated polymerization (NMP)[9] have provided wide access to a range of materials, with complex architectures and numerous properties. Among the beneficial aspects of RDRP techniques has been their versatility when different conditions (solvents, range of temperatures and monomer types) are required. However, for the case of acrylamides, copper-mediated RDRP has often exhibited difficulties to conduct, especially in aqueous media.[10-12]

Although the synthesis of poly(acrylamides) by living radical polymerisation methods has proven to be difficult, it has been facilitated with the use of the pre-disproportionation of Cu(I) in water under appropriate conditions. The presence of a multidentate aliphatic amine as the ligand usually greatly stabilizes Cu(II) in aqueous environments, eventually leading to controlled and rapid Cu-RDRP.[13-16] Moreover, Cu(I) in the presence of aliphatic multidentate tertiary amine ligands such as Me_6TREN is unstable towards rapid disproportionation and, thus contrary to some recent reports, many copper(I) ATRP catalysts are very unstable in water and aqueous environments.[17] This instability can be exploited as long as sufficient time (usually < 1 minute) is allowed for full disproportionation prior

to monomer addition. The resulting mixture of Cu(0) and Cu(II) species in water gives effective and controlled polymerisation of water soluble acrylates and acrylamides. As a result, different acrylamide monomers can be used for the synthesis of homopolymers. The robustness of this aqueous-mediated Cu-RDRP has been demonstrated through its implementation under bio-friendly conditions for the generation of polymer-protein conjugates.[18] The mild conditions applied (*i.e.* low temperature), enables the utilization of monomers such as *N*-isopropylacrylamide (NiPAm) which leads to polymers with LCST transitions giving access to the facile synthesis of temperature-responsive materials.[19]

A challenge that arises from the aqueous mediated Cu-RDRP of acrylamides is the potential for side reactions. These are related to the instability of the deactivator, the hydrolysis of the alkyl halide chain end, or the conventional radical–radical termination.[10, 14, 20, 21] The hydrolysis of the alkyl halide in particular can be detrimental since the occurring hydroxyl-terminated polymers are inefficient to participate in co-polymerizations depending upon the timescale of the hydrolysis relative to propagation.[12] As a result, the preparation of polyacrylamide block copolymers has been limited when Cu-RDRP in aqueous media is used. Perrier and co-workers have reported the RAFT polymerisation of up to icosa-block copolymer (20 blocks) in both organic and aqueous media.[22-24] Although highly efficient, this approach was applied at relatively high temperature (~70 ^{o}C), limiting the monomer choice and the potential of biomolecules to be involved in the polymerization under the reaction conditions. The properties of light as continuously applied external stimuli has been demonstrated by Junkers and colleagues who employed photoinitiated Cu-RDRP in water-ethanol mixtures for the synthesis of a decablock copolymer.[25] We have previously used the pre-disproportionation of Cu(I)Br in water, and in the presence of the aliphatic amine Me_6Tren as ligand, for the rapid synthesis of polyacrylamide multiblock homopolymers and copolymers.[13, 26] However, in both cases, the targeted degrees of polymerization were confined to DP_n = 10-80 and the molecular weights obtained were low. As a result, the synthesis of higher molecular weight polyacrylamide block copolymers has not been developed with the existing approaches having been limited to either mixtures of organic-aqueous media or low molar masses.

Despite the synthetic challenges, many polyacrylamide-based materials display diverse properties important for a wide range of application such as oil recovery,[27] water treatment,[28] biochemistry and drug delivery systems.[19, 29, 30] In particular, poly(*N*-isopropyl acrylamide) (PNiPAm) is arguably one of the most popular materials for the thermal properties that exhibits, due to its lower critical solution temperature (LCST) at 32 ^{o}C. This particular characteristic of PNiPAm has attracted a lot of interest since it gives the ability to tune the LCST and viscosity of PNiPAm-based polymeric systems in aqueous solutions.[31-34] As such, the combination of PNiPAm with polymers of different hydrophilicity/hydrophobicity allows for the design of polymeric materials with a range of applications.[35, 36]

Herein, we report the rapid synthesis of well-defined higher molecular weight (M_n ~ 30 k) PNiPAM-*b*-PHEAAm block copolymers through Cu-RDRP in aqueous media, utilizing the pre-disproportionation of Cu(I)Br in the presence of Me_6Tren. The versatility of the technique allowed for the design of the block ratio, with each block comprising up to 100 monomer units. The well-defined block copolymers exhibited thermo-switchable properties dependent on the ratio between the segments and temperature alterations. The thermo-induced aggregation phenomena were examined through DLS and fluorescence measurements after employing the fluorescent probe Nile Red. Moreover, the viscosity phenomena dependent on the PHEAAm contribution were studied through viscometry, and insights on the thermal stability of the copolymers were obtained through thermal analysis.

Results and Discussion

Initial experiments focussed on the synthesis of the diblock copolymer PNiPAm$_{100}$-*b*-PHEAAm$_{100}$. Following previous literature,[14, 26] the synthesis of the first block was carried out with [NiPAm]:[I]:[Cu(I)Br]:[Me$_6$Tren]=[100]:[1]:[0.8]:[0.4]. Firstly, the disproportionation of Cu(I) took place within < 1 minute to give a blue solution and a black precipitate, in water and in the presence of the tertiary amine Me$_6$Tren as ligand and Cu(I)Br as copper source, exploiting the instability of Cu(I) in water. Subsequently, the aqueous solution of the first monomer (NiPAm) and the initiator (2,3-dihydroxypropyl 2-bromo-2-methylpropanoate) was added to this blue solution and the polymerization was left to commence in a N_2-deoxygenated environment (**Scheme 1**). As reported, the good control over the Cu-RDRP in aqueous media is highly dependent on the ratio between Cu(I)Br and Me$_6$Tren which, for targeted DP 100 for both blocks, was maintained 2:1 throughout the polymerization. One of the most important factors for the efficient synthesis of block copolymers *via* sequential monomer addition is the need for high end-group fidelity of the first block, namely the homopolymer. On account of this, a prolonged residency of the homopolymer in the aqueous reaction media was avoided, in order to limit the nucleophilic substitution of the *ω*-Br by H_2O, and when the homopolymerization of NiPAm reached near-quantitative conversion (~99%) (**Figure S1**&**S2**) the second monomer (HEAAm) was promptly added. The resulting diblock copolymer was obtained in a controlled manner, exhibiting agreement between theoretical ($M_{n,th.}$~ 23,000) and experimental ($M_{n,SEC}$ ~30,000) M_n values (), as well as low dispersity ($Đ$ ~1.08) in very high conversion ~ 99 % (**Figure 1a**, **Figure S3**, **Table 1-**entry 5). It is noted here that the values reported are reportedwith respect to PMMA narrow molecular weight standards used for the calibration of SEC. In the analysis, we have used the Mark Houwink constants for PMMA and no universal calibration corrections have been applied. We have deliberately analysed in this way, as the polymers produced will have very different radii of gyration in the eluent used. This will especially be true for the block copolymers and thus formed the basis of the decision to treat all in the same way and in a way that would be easily reproducible by other laboratories should they choose to repeat this work.

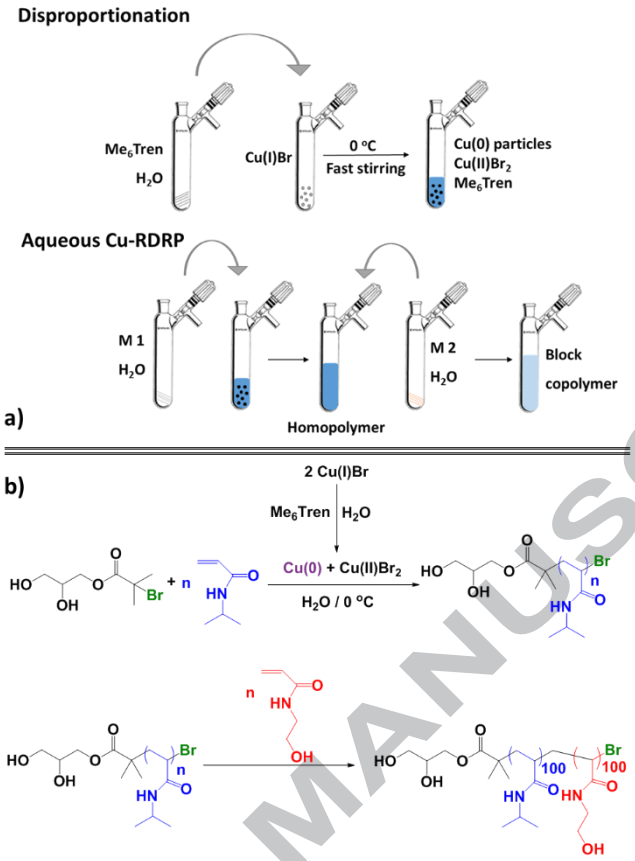

Scheme 1. Schematic representation of **a)** the reaction setup for the aqueous Cu-RDRP *via* predisproportionation of Cu(I)Br/Me_6Tren in water and **b)** the reactions for the synthesis of $PNiPAm_x$-*b*-$PHEAAm_y$ block copolymers.

In order to examine the ability to design the composition of the two blocks, a series of diblock copolymers with different ratios of PNiPAm and PHEAAm were targeted. Diblock copolymers with various segment ratios were obtained in a controlled manner, exhibiting narrow dispersities ($Đ$=1.13-1.22) and controlled molecular weights ($M_{n,SEC}$~30 k, given the caveat on differences in radii of gyration for the different polymers) in near-full conversions (>99%) (**Table 1**-entries 1-4, 7-10**, Figure 1b-f, Figure S4**). Apart from the diblock copolymer $PNiPAm_{100}$-*b*-$PHEAAm_{100}$ (**Figure 1a**), a random copolymer with equal molar equivalents of PNiPAm and PHEAAm was synthesized (**Figure S6, Table 1**-entry 6), resulting in similar molecular characteristics to the diblock copolymer, thus with a slightly increased dispersity ($Đ$~1.20).

Table 1. ^{1}H NMR and SEC analysis for the synthesized PNiPAm-PHEAAm copolymers with different block ratios.

Entry	Polymer	$M_{n,SEC}$ [a]	$M_{n,th}$ (g/mol)	$Đ$	Conversion ^{1}H NMR (%)
1	PNiPAm$_{180}$-*b*-PHEAAm$_{20}$	30,900	23,000	1.14	>99
2	PNiPAm$_{160}$-*b*-PHEAAm$_{40}$	29,300	23,000	1.16	>99
3	PNiPAm$_{140}$-*b*-PHEAAm$_{60}$	30,000	23,000	1.13	>99
4	PNiPAm$_{120}$-*b*-PHEAAm$_{80}$	30,500	23,000	1.21	>99
5[b]	PNiPAm$_{100}$-*b*-PHEAAm$_{100}$	30,000	23,000	1.08	>99
6[c]	PNiPAm$_{100}$-PHEAAm$_{100}$	29,300	23,000	1.21	>99
7	PNiPAm$_{80}$-*b*-PHEAAm$_{120}$	30,800	23,000	1.16	>99
8	PNiPAm$_{60}$-*b*-PHEAAm$_{140}$	30,600	23,000	1.22	>99
9	PNiPAm$_{40}$-*b*-PHEAAm$_{160}$	29,600	23,000	1.21	>99
10	PNiPAm$_{20}$-*b*-PHEAAm$_{180}$	30,300	23,000	1.13	>99

[a] Determined by DMF SEC analysis and expressed as molecular weight equivalents to PMMA narrow molecular weight standards. [b] Block copolymer and [c] random copolymer.

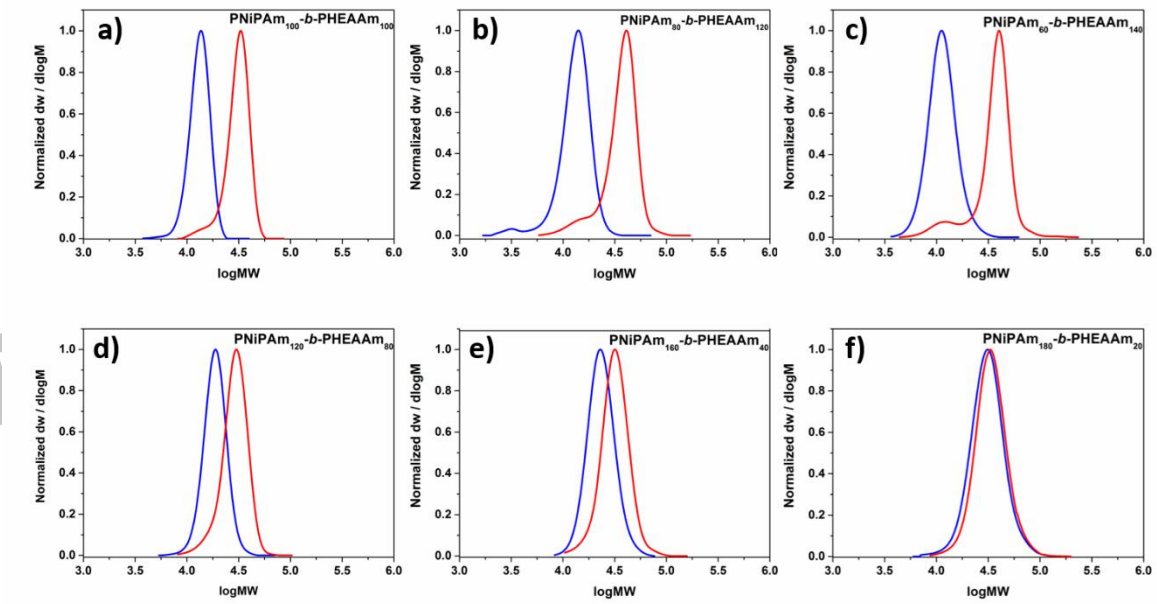

Figure 1: SEC traces of PNiPAm$_x$-*b*-PHEAAm$_y$ copolymers with different segment ratios with **a)** PNiPAm$_{100}$-*b*-PHEAAm$_{100}$, **b)** PNiPAm$_{80}$-*b*-PHEAAm$_{120}$, **c)** PNiPAm$_{60}$-*b*-PHEAAm$_{140}$, **d)** PNiPAm$_{120}$-*b*-PHEAAm$_{80}$, **e)** PNiPAm$_{160}$-*b*-PHEAAm$_{40}$, **f)** PNiPAm$_{180}$-*b*-PHEAAm$_{20}$.

Although PNiPAm is a well-established thermo-responsive polymer, the investigation of its behaviour on different applications is still developing, finding applications from drug delivery[19] to oilfield operations.[37] Based on this, we were interested in the thermo-responsive properties of the obtained $PNiPAm_{100}$-*b*-$PHEAAm_{100}$. Initially, the diblock copolymer was exposed to a range of temperatures (30-65 ^{o}C). Although the lower critical solution temperature (LCST) phase transition of PNiPAm is 32 ^{o}C,[31, 38, 39] upon exposure at temperatures above 50 ^{o}C the $PNiPAm_{100}$-*b*-$PHEAAm_{100}$ diblock copolymer did not display any noticeable phase transitions, but did exhibit an increase in the viscosity. This was attributed to the presence of the hydrophilic PHEAAm block, which perpetuated the hydrophilicity of the diblock, alternating the aggregation behaviour of PNiPAm, preventing its phase transition, thus leading to a solution with high viscosity, a phenomenon which was reversible upon cooling (**Figure 2b**&**c**). However, when the diblock copolymers with various segment ratios were examined, different viscosity behaviours were observed. In particular, the diblock copolymers with molar ratios close to 50% PNiPAm and 50% PHEAAm exhibited the highest viscosity, while when either of the hydrophilic or the hydrophobic segments was predominant (molar ratio ≥80 % for each case), these viscosity phenomena were not observed (**Figure 2a**). This is attributed to the phase transition phenomena occurring when the PNiPAm is mainly present or, on the contrary, the high hydrophilicity derived from the PHEAAm segment when the latter consists more than 80% of the diblock. Noteworthy is that the random copolymer did not present the same viscosity behaviour as the diblock (**Figure S6**). As a result, both the structure and the composition of the copolymers affect their temperature-responsive behaviour. In order to further understand our findings, the effect of the PHEAAm segment on the LCST of PNiPAm was examined through turbidity measurements. It was shown that the increase of the hydrophilic PHEAAm segment in the copolymers increased the LCST of the copolymers caused by the PNiPAm segment, while for the case of $PNiPAm_{100}$-*b*-$PHEAAm_{100}$ with 1:1 molar ratio, no LCST was evident (**Figure S7**).

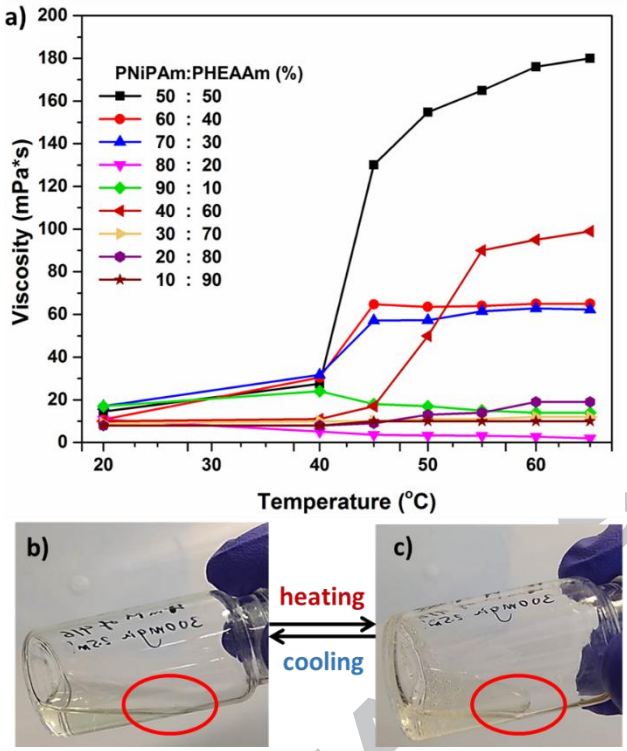

Figure 2. a) Viscosity values at different temperatures for the PNiPAm$_x$-*b*-PHEAAm$_y$ copolymers with different segment ratios and illustration of the reversible high viscosity phenomenon observed for the PNiPAm$_{100}$-*b*-PHEAAm$_{100}$ block copolymer **b)** upon heating and **c)** upon cooling.

Since the PNiPAm$_{100}$-*b*-PHEAAm$_{100}$ polymer consists of a relatively hydrophobic (PNiPAm) and a hydrophilic (PHEAAm) segment, its aggregation in water was examined through encapsulation of the fluorescent probe Nile Red, which upon excitation with λ = 550 nm light results in low fluorescence with λ_{max} = 650 nm. When the dye resides in a hydrophobic environment, such as the interior of a micelle in aqueous media, the resulting fluorescence increases markedly. As such, aqueous solutions of PNiPAm$_{100}$-*b*-PHEAAm$_{100}$ in different concentrations were treated with Nile Red and incubated for 2 hours to allow for encapsulation of the dye. The resulting fluorescence emission spectra revealed a shift in the wavelength maximum for the dye, from 650 nm to ~627 nm, indicating the presence of aggregates. More specifically, as the concentration of the diblock increased, the emission intensity also gradually increased, indicating a steady aggregate formation (**Figure 3a**). The inflection point in λ_{max} revealed the critical aggregation concentration (CAC) which was found to be 0.18 mg/mL (**Figure 3b**). Below the CAC the rise in absorbance is weak, indicating a low concentration of aggregates while above the found CAC the absorbance increase is highly evident. Subsequently, we were interested in determining the effect of temperature on the aggregation behaviour of the obtained diblock copolymer. For this purpose fluorescence measurements were measured as previously, over a range of temperatures (30-65 ^{o}C) for PNiPAm$_{100}$-*b*-PHEAAm$_{100}$ in 1 mg/mL concentration (**Figure 3c**). The resulting spectra revealed a shift in the λ_{max} and a predominant intensity increase above 50 ^{o}C. The temperature above which the aggregation formation is highly observed (herein mentioned critical aggregation temperature, CAT) was found to be 53 ^{o}C (**Figure 3d**).

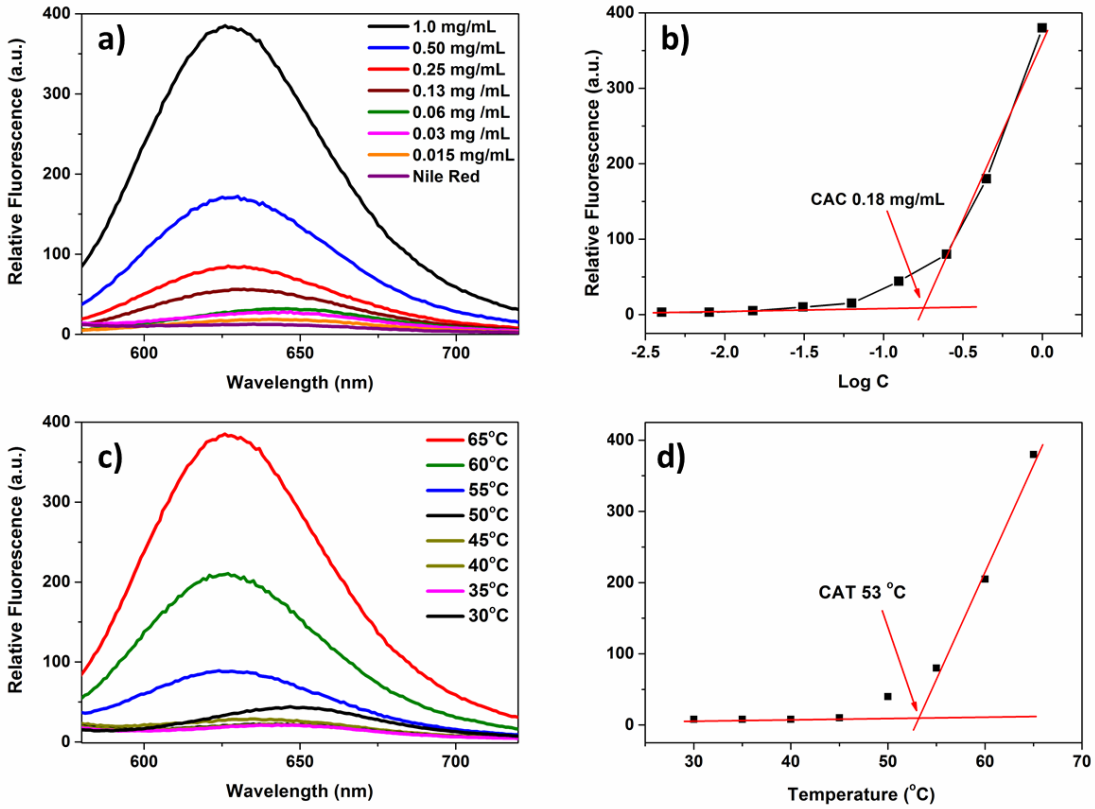

Figure 3. a) Fluorescence measurements of Nile Red encapsulated in PNiPAm$_{100}$-*b*-PHEAAm$_{100}$ of varying concentrations at 70 °C and **b)** determination of the critical aggregation concentration (CAC) as 0.18 mg/mL, **c)** Emission spectra of Nile Red encapsulated in 1 mg/mL PNiPAm$_{100}$-*b*-PHEAAm$_{100}$ at various temperatures and **d)** determination of the critical aggregation temperature (CAT) as 53 °C.

In order to further corroborate our findings on the aggregate formation, dynamic light scattering (DLS) measurements were conducted. Initially, the homopolymer PNiPAm was measured at a range of temperatures (20-70 °C). For temperatures below, or very close to, the LCST of PNiPAm, 20-33 °C, the DLS measurements showed a relatively narrow size distribution of ~ 5 nm for the PNiPAm, while when the homopolymer was heated to temperatures above its LCST (34-70 °C), the size distribution of the hydrodynamic diameters (R_h) changed dramatically, resulting in aggregates with bigger size (~200 nm) (**Figure 4a&b, Figure S8, Table S1**). This was attributed to hydrophobic interactions between the PNiPAm chains, leading to hydrophobic collapse at T>LCST. The DLS measurements for the diblock copolymer revealed different size distribution values. When temperatures below the found CAT were applied (T <53°C) the size distribution ranged from 10 to 30 nm, while at T>53 °C, a clear shift to larger sizes was evident, thus still smaller than the homopolymer's results (**Figure 4a&b, Figure S9, Table S1**). This was attributed to the role of the PHEAAm which preserves the hydrophilicity and prevents the hydrophobic collapse of the diblock. However, the shift to larger and broader size distributions at 60 °C and 70 °C, might be attributed to intermicellar hydrophobic interactions that occur mainly above the CAT. [40] Conversely, when the statistical copolymer was examined by DLS, it only resulted in a population of 10-30 nm with a sharp distribution for the whole range of temperatures (**Figure 4a&b, Figure S10, Table S1**,). Based on the DLS findings, there is a clear structural effect on the aggregation behaviour of the PNiPAm$_x$-*b*-PHEAAm$_y$, which is highly evident when the random and the diblock copolymers are compared. This comes in agreement with

our findings on the high viscosity phenomenon, which is only present for the diblock, whereas the random copolymer remains slightly viscous at any temperature. Consequently, the size of the aggregates can be tuned by altering the PHEAAm segment at the preferred temperature.

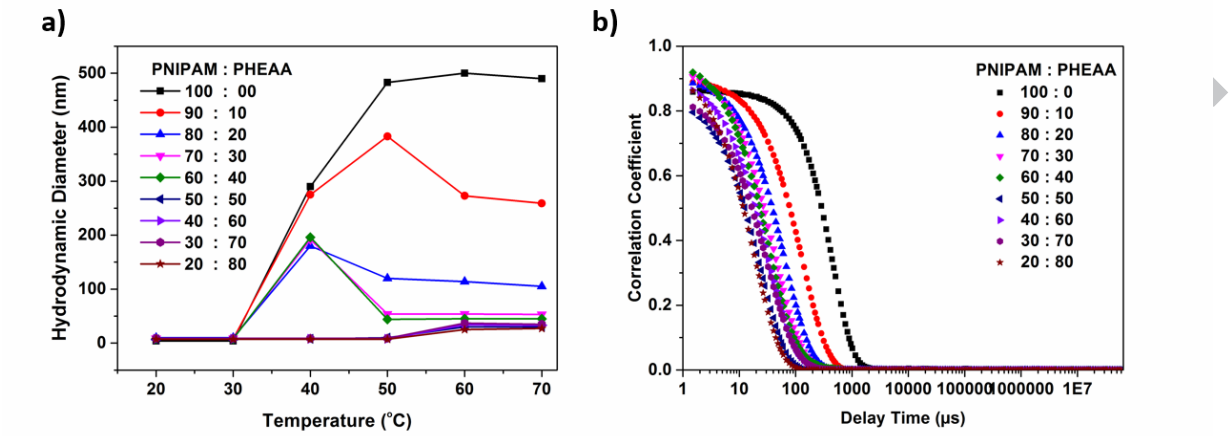

Figure 4. a) Illustration of the hydrodynamic diameter values at different temperatures and **b)** DLS measured correlation curves for the different diblock copolymers.

Conclusion

In summary, we report the controlled and rapid synthesis of a series of PNiPAm$_x$-*b*-PHEAAm$_y$ block copolymers through Cu-RDRP in water with temperature-responsive behaviour. The copolymers exhibited aggregation and thermo-switchable properties dependent not only on temperature variations but also on the ratio between the segments of the blocks, which could be precisely controlled. Thermal analyses revealed that this thermo-switchable nature was highly evident for the PNiPAm$_{100}$-*b*-PHEAAm$_{100}$ diblock copolymer, which, at specific temperature exhibited reversible high viscosity phenomena and loss of LCST. The sharp temperature-induced reversible large increases in viscosity/gelation rendering theseblock copolymers as potential candidates for temperature-dependent applications, such as oil-recovery and personal care.

The raw/processed data required to reproduce these findings cannot be shared at this time as the data also forms part of an ongoing study.

Acknowledgements

We appreciate financial support from the University of Warwick and King Abdulaziz City for Science and Technology (KACST). Equipment used in this research was supported by the University of Warwick RTP in Polymer Characterisation.

References

1. M. Kato, M. Kamigaito, M. Sawamoto and T. Higashimura, *Macromolecules*, 1995, **28**, 1721-1723.
2. J.-S. Wang and K. Matyjaszewski, *J. Am. Chem. Soc.*, 1995, **117**, 5614-5615.
3. V. Percec, T. Guliashvili, J. S. Ladislaw, A. Wistrand, A. Stjerndahl, M. J. Sienkowska, M. J. Monteiro and S. Sahoo, *J. Am. Chem. Soc.*, 2006, **128**, 14156-14165.
4. B. M. Rosen and V. Percec, *Chem. Rev.*, 2009, **109**, 5069-5119.
5. A. Anastasaki, V. Nikolaou, G. Nurumbetov, P. Wilson, K. Kempe, J. F. Quinn, T. P. Davis, M. R. Whittaker and D. M. Haddleton, *Chem. Rev.*, 2016, **116**, 835-877.
6. J. Chiefari, Y. K. Chong, F. Ercole, J. Krstina, J. Jeffery, T. P. T. Le, R. T. A. Mayadunne, G. F. Meijs, C. L. Moad, G. Moad, E. Rizzardo and S. H. Thang, *Macromolecules*, 1998, **31**, 5559-5562.
7. S. Perrier, *Macromolecules*, 2017, **50**, 7433-7447.
8. C. Barner-Kowollik, T. P. Davis, J. P. A. Heuts, M. H. Stenzel, P. Vana and M. Whittaker, *J. Polym. Sci., Part A: Polym. Chem.*, 2003, **41**, 365-375.
9. C. J. Hawker, A. W. Bosman and E. Harth, *Chem. Rev.*, 2001, **101**, 3661-3688.
10. G. R. Jones, A. Anastasaki, R. Whitfield, N. Engelis, E. Liarou and D. M. Haddleton, *Angew. Chem. Int. Ed.*, 2018, **57**, 10468-10482.
11. M. Teodorescu and K. Matyjaszewski, *Macromolecules*, 1999, **32**, 4826-4831.
12. J. T. Rademacher, M. Baum, M. E. Pallack, W. J. Brittain and W. J. Simonsick, *Macromolecules*, 2000, **33**, 284-288.
13. G. R. Jones, Z. Li, A. Anastasaki, D. J. Lloyd, P. Wilson, Q. Zhang and D. M. Haddleton, *Macromolecules*, 2016, **49**, 483-489.
14. Q. Zhang, P. Wilson, Z. Li, R. McHale, J. Godfrey, A. Anastasaki, C. Waldron and D. M. Haddleton, *J. Am. Chem. Soc.*, 2013, **135**, 7355-7363.
15. C. Waldron, Q. Zhang, Z. Li, V. Nikolaou, G. Nurumbetov, J. Godfrey, R. McHale, G. Yilmaz, R. K. Randev, M. Girault, K. McEwan, D. M. Haddleton, M. Droesbeke, A. J. Haddleton, P. Wilson, A. Simula, J. Collins, D. J. Lloyd, J. A. Burns, C. Summers, C. Houben, A. Anastasaki, M. Li, C. R. Becer, J. K. Kiviaho and N. Risangud, *Polym. Chem.*, 2014, **5**, 57-61.
16. D. J. Lloyd, V. Nikolaou, J. Collins, C. Waldron, A. Anastasaki, S. P. Bassett, S. M. Howdle, A. Blanazs, P. Wilson, K. Kempe and D. M. Haddleton, *Chem. Commun.*, 2016, **52**, 6533-6536.
17. F. A. Cotton and G. Wilkinson, *Advanced inorganic chemistry*, Wiley New York, 1988.
18. Q. Zhang, M. Li, C. Zhu, G. Nurumbetov, Z. Li, P. Wilson, K. Kempe and D. M. Haddleton, *J. Am. Chem. Soc.*, 2015, **137**, 9344-9353.
19. E. Liarou, S. Varlas, D. Skoulas, C. Tsimblouli, E. Sereti, K. Dimas and H. Iatrou, *Prog. Polym. Sci.*, 2018, **83**, 28-78.
20. M. Fantin, A. A. Isse, A. Gennaro and K. Matyjaszewski, *Macromolecules*, 2015, **48**, 6862-6875.
21. F. Alsubaie, A. Anastasaki, V. Nikolaou, A. Simula, G. Nurumbetov, P. Wilson, K. Kempe and D. M. Haddleton, *Macromolecules*, 2015, **48**, 6421-6432.
22. G. Gody, T. Maschmeyer, P. B. Zetterlund and S. Perrier, *Macromolecules*, 2014, **47**, 639-649.
23. G. Gody, T. Maschmeyer, P. B. Zetterlund and S. Perrier, *Nat. Commun.*, 2013, **4**, 2505.
24. G. Gody, T. Maschmeyer, P. B. Zetterlund and S. Perrier, *Macromolecules*, 2014, **47**, 3451-3460.
25. Y.-M. Chuang, A. Ethirajan and T. Junkers, *ACS Macro Lett.*, 2014, **3**, 732-737.
26. F. Alsubaie, A. Anastasaki, P. Wilson and D. M. Haddleton, *Polym. Chem.*, 2015, **6**, 406-417.
27. A. Z. Abidin, T. Puspasari and W. A. Nugroho, *Procedia Chem.*, 2012, **4**, 11-16.
28. S. S. Wong, T. T. Teng, A. L. Ahmad, A. Zuhairi and G. Najafpour, *J. Hazard. Mater.*, 2006, **135**, 378-388.
29. H. Schägger and G. von Jagow, *Anal. Biochem.*, 1987, **166**, 368-379.
30. V. Raus and L. Kostka, *Polym. Chem.*, 2019, **10**, 564-568.

31. A. Saeed, D. M. R. Georget and A. G. Mayes, *React. Funct. Polym.*, 2010, **70**, 230-237.
32. C. Monteux, R. Mangeret, G. Laibe, E. Freyssingeas, V. Bergeron and G. Fuller, *Macromolecules*, 2006, **39**, 3408-3414.
33. A. J. Howe, A. M. Howe and A. F. Routh, *J. Colloid Interface Sci.*, 2011, **357**, 300-307.
34. Q.-T. Pham, Z.-H. Yao, Y.-T. Chang, F.-M. Wang and C.-S. Chern, *J. Taiwan Inst. Chem. Eng.*, 2018, **93**, 63-69.
35. X.-M. Liu, L.-S. Wang, L. Wang, J. Huang and C. He, *Biomaterials*, 2004, **25**, 5659-5666.
36. X.-M. Liu, K. P. Pramoda, Y.-Y. Yang, S. Y. Chow and C. He, *Biomaterials*, 2004, **25**, 2619-2628.
37. L. Ree, M. A. Kelland, D. Haddleton and F. Alsubaie, *Energy Fuels*, 2017, **31**, 1355-1361.
38. H. G. Schild, *Prog. Polym. Sci.*, 1992, **17**, 163-249.
39. L. M. Geever, D. M. Devine, M. J. D. Nugent, J. E. Kennedy, J. G. Lyons, A. Hanley and C. L. Higginbotham, *Eur. Polym. J.*, 2006, **42**, 2540-2548.
40. S.-T. Lin, K. Fuchise, Y. Chen, R. Sakai, T. Satoh, T. Kakuchi and W.-C. Chen, *Soft Matter*, 2009, **5**, 3761-3770.

Highlights

- Synthesis of acrylamide diblock copolymers via aqueous Cu-RDRP with high molecular weights, low dispersities and quantitative conversions.
- Control over the polymerization enables the design of diblock copolymers with different segment ratio.
- Diblock copolymers with specific composition exhibit thermo-responsive aggregation and viscosity.
- Thermal analysis, fluorescent measurements, DLS and viscometry provide information about the thermal stability, thermo-responsive viscosity and aggregation behaviour of the diblock copolymers in aqueous media.

Graphical abstract